






Communication

# Synthesis and In Vitro Evaluation of Novel Dopamine Receptor D<sub>2</sub> 3,4-dihydroquinolin-2(1H)-one Derivatives Related to Aripiprazole

Radomir Juza<sup>1,2</sup>, Kristyna Stefkova<sup>1</sup>, Wim Dehaen<sup>3</sup>, Alena Randakova<sup>4</sup>, Tomas Petrasek<sup>1</sup>, Iveta Vojtechova<sup>1</sup> , Tereza Kobrlova<sup>5</sup>, Lenka Pulkrabkova<sup>5</sup>, Lubica Muckova<sup>5</sup> , Marko Mecava<sup>5</sup>, Lukas Prchal<sup>5</sup>, Eva Mezeiova<sup>1,5</sup> , Kamil Musilek<sup>2</sup> , Ondrej Soukup<sup>5,\*</sup> and Jan Korabecny<sup>1,5,\*</sup> 

<sup>1</sup> National Institute of Mental Health, Topolova 748, 250 67 Klecany, Czech Republic; juza25@seznam.cz (R.J.); Kristyna.Stefkova@nudz.cz (K.S.); tomas.petrasek@nudz.cz (T.P.); vojtechova.Iveta@seznam.cz (I.V.); eva.mezeiova@gmail.com (E.M.)

<sup>2</sup> Department of Chemistry, University of Hradec Kralove, Rokitanskeho 62, 500 03 Hradec Kralove, Czech Republic; kamil.musilek@uhk.cz

<sup>3</sup> CZ-OPENSREEN: National Infrastructure for Chemical Biology, Department of Informatics and Chemistry, Faculty of Chemical Technology, University of Chemistry and Technology Prague, Technicka 5, 166 28 Prague, Czech Republic; wimdehaen@gmail.com

<sup>4</sup> Institute of Physiology, Czech Academy of Sciences, Videnska 1083, 142 20 Prague, Czech Republic; Alena.Randakova@fgu.cas.cz

<sup>5</sup> Biomedical Research Centre, University Hospital Hradec Kralove, Sokolska 581, 500 05 Hradec Kralove, Czech Republic; kobrlova.tereza@gmail.com (T.K.); lenka.pulkrabkova@fnhk.cz (L.P.); lubica.muckova@unob.cz (L.M.); markomecava@centrum.cz (M.M.); lukas.prchal@fnhk.cz (L.P.)

\* Correspondence: ondrej.soukup@fnhk.cz (O.S.); jan.korabecny@fnhk.cz (J.K.); Tel.: +420-495-833-447 (O.S.); +420-973-255-167 (J.K.)



**Citation:** Juza, R.; Stefkova, K.; Dehaen, W.; Randakova, A.; Petrasek, T.; Vojtechova, I.; Kobrlova, T.; Pulkrabkova, L.; Muckova, L.; Mecava, M.; et al. Synthesis and In Vitro Evaluation of Novel Dopamine Receptor D<sub>2</sub> 3,4-dihydroquinolin-2(1H)-one Derivatives Related to Aripiprazole. *Biomolecules* **2021**, *11*, 1262. <https://doi.org/10.3390/biom11091262>

Academic Editors: Marco Bortolato and Simona Scheggi

Received: 15 July 2021

Accepted: 20 August 2021

Published: 24 August 2021

**Publisher's Note:** MDPI stays neutral with regard to jurisdictional claims in published maps and institutional affiliations.



**Copyright:** © 2021 by the authors. Licensee MDPI, Basel, Switzerland. This article is an open access article distributed under the terms and conditions of the Creative Commons Attribution (CC BY) license (<https://creativecommons.org/licenses/by/4.0/>).

**Abstract:** In this pilot study, a series of new 3,4-dihydroquinolin-2(1H)-one derivatives as potential dopamine receptor D<sub>2</sub> (D<sub>2</sub>R) modulators were synthesized and evaluated in vitro. The preliminary structure–activity relationship disclosed that compound **5e** exhibited the highest D<sub>2</sub>R affinity among the newly synthesized compounds. In addition, **5e** showed a very low cytotoxic profile and a high probability to cross the blood–brain barrier, which is important considering the observed affinity. However, molecular modelling simulation revealed completely different binding mode of **5e** compared to USC-D301, which might be the culprit of the reduced affinity of **5e** toward D<sub>2</sub>R in comparison with USC-D301.

**Keywords:** aripiprazole; dopamine receptor; blood–brain barrier; molecular modeling studies; schizophrenia

## 1. Introduction

Dopamine primarily mediates its effect through activation of dopamine receptors (DRs) [1]. There are a total of five DR subtypes that are members of the G-protein-coupled receptors (GPCRs) [2], and are further divided into two classes according to the structure. The D<sub>1</sub>-like family includes D<sub>1</sub>Rs and D<sub>5</sub>Rs, whereas D<sub>2–4</sub>Rs belong to the D<sub>2</sub>-like family [1–3]. The main difference between both families is that D<sub>1</sub>-like family activate adenylate cyclase (AC), which leads to production of cyclic adenosine monophosphate (cAMP), whereas D<sub>2</sub>-like stimulates AC activity.

Dopamine D<sub>2</sub> type receptors (D<sub>2</sub>Rs) are integral membrane receptors coupled to G proteins with three extracellular loops, seven transmembrane domains, and three intracellular loops [4,5]. D<sub>2</sub>Rs are present in two isoforms, short D<sub>2S</sub> and long D<sub>2L</sub>, which differ by the insertion of 29 amino acids in the third intracellular loop on D<sub>2L</sub>Rs [6]. The “short” version is exclusively expressed presynaptically as an autoreceptor, whereas, the “long” one is mainly found at the postsynaptic cells [7]. Furthermore, both isoforms can inhibit intracellular cyclic adenosine monophosphate via G<sub>i</sub> [4]. The highest levels of D<sub>2</sub>Rs in the human brain are expressed within striatum, the olfactory tubercle, and the nucleus

accumbens, but it can be also found in the ventral tegmental area, substantia nigra, septum, amygdala, cortical areas, and hippocampus. D<sub>2</sub>Rs are involved in working memory, reward motivation functions, and regulation of locomotion [2,8]. D<sub>2</sub>Rs are the main target in the treatment of schizophrenia [9]. Indeed, antagonists or partial agonists of D<sub>2</sub>Rs are the main representatives for schizophrenia. Besides, they can be applied in the therapy of depression and anxiety [9–13].

Schizophrenia is a serious mental disorder that affects up to 1% of the population worldwide [9]. It is believed, that environmental factors (i.e., viral infection, early childhood trauma, and obstetrical complications) increase the expression of certain genes to enhance risk factors for schizophrenia out-break [14,15]. The symptoms of schizophrenia include three groups, namely (i) positive (hallucinations, disorganized speech and delusions), (ii) negative (diminished expressiveness and reduced motivation), and (iii) cognitive (impaired memory, decreased speed of mental processing and executive functions) [14]. The pathophysiology of schizophrenia is poorly understood, however, it is assumed, that dysfunction of the dopamine mesolimbic pathway is responsible for positive symptoms and mesocortical pathway for negative symptoms [9,16]. Cognitive symptoms have been suggested to result from decreased levels of dopamine in cortical areas [17]. The current approaches for the management of schizophrenia involve three generations of antipsychotics. The first antipsychotics are mainly D<sub>2</sub>R antagonists, the second exhibit multi-target antagonism with significant antagonism at serotonin 5-HT<sub>2A</sub> type receptor (5-HT<sub>2A</sub>R), and the third possess a multi-target profile with partial agonism at D<sub>2</sub>R [9]. All licensed neuroleptics exhibited D<sub>2</sub>R affinity at therapeutic doses crucial for their mechanism of action [18–21]. In addition to D<sub>2</sub>Rs affinity, antipsychotic drugs show activity toward other dopamine (D<sub>1</sub>, D<sub>3</sub>, and D<sub>4</sub>) and serotonin (especially 5-HT<sub>1A</sub>, 5-HT<sub>2A</sub>, and 5-HT<sub>2C</sub>) receptors. However, selective D<sub>1</sub>, D<sub>3</sub>, and D<sub>4</sub> receptor antagonists are not so effective in providing antipsychotic response, and D<sub>1</sub>Rs agonists exhibited limited clinical efficacy [22–27]. The evidence of 5-HT<sub>1A</sub>Rs agonism/partial agonism is inconclusive and the role of the 5-HT<sub>2A</sub>Rs antagonism is neither necessary nor a major contributor to antipsychotic effect [28–30]. Furthermore, 5-HT<sub>2C</sub>Rs antagonism has been associated mainly with side-effects including weight gain, diabetes, and sexual disturbances [30,31]. On the other hand, pimavanserin (an inverse agonist at 5-HT<sub>2A</sub>Rs) has recently been approved for the treatment of psychosis associated with Parkinson's disease [32]. According to various studies, there is no benefit even when choosing different combinations of antipsychotics in 13–50% of all patients [33]. In addition, the current medication reduces mainly positive symptoms and causes severe side-effects such as diabetes, sexual dysfunction, weight gain, confusion, blurred vision, sedation, or dizziness, which also typically occurs during the treatment of depressive or anxiety disorders [34–38]. Thus, there is an enormous need to develop new effective and safe neuroleptic drugs since CNS disorders are also considered among the most expensive medical conditions (the total cost of disorders of the brain was estimated 798 billion EUR in Europe in 2010) [39].

In this pilot study, we designed and synthesized a novel series of compounds based on the approved drug aripiprazole characterized by the effect via D<sub>2</sub>R [40], in combination with structural properties of USC-D301, highly selective D<sub>2</sub>R ligand [41]. Considering this effect, we have performed in vitro evaluation of novel 3,4-dihydroquinolin-2(1H)-one derivatives (Figure 1) for their affinity to D<sub>2</sub>Rs, predicted their CNS availability, and established their cytotoxicity profile in order to estimate the clinical relevance of our observations. The D<sub>2</sub>Rs affinity is also corroborated by the in silico simulation.

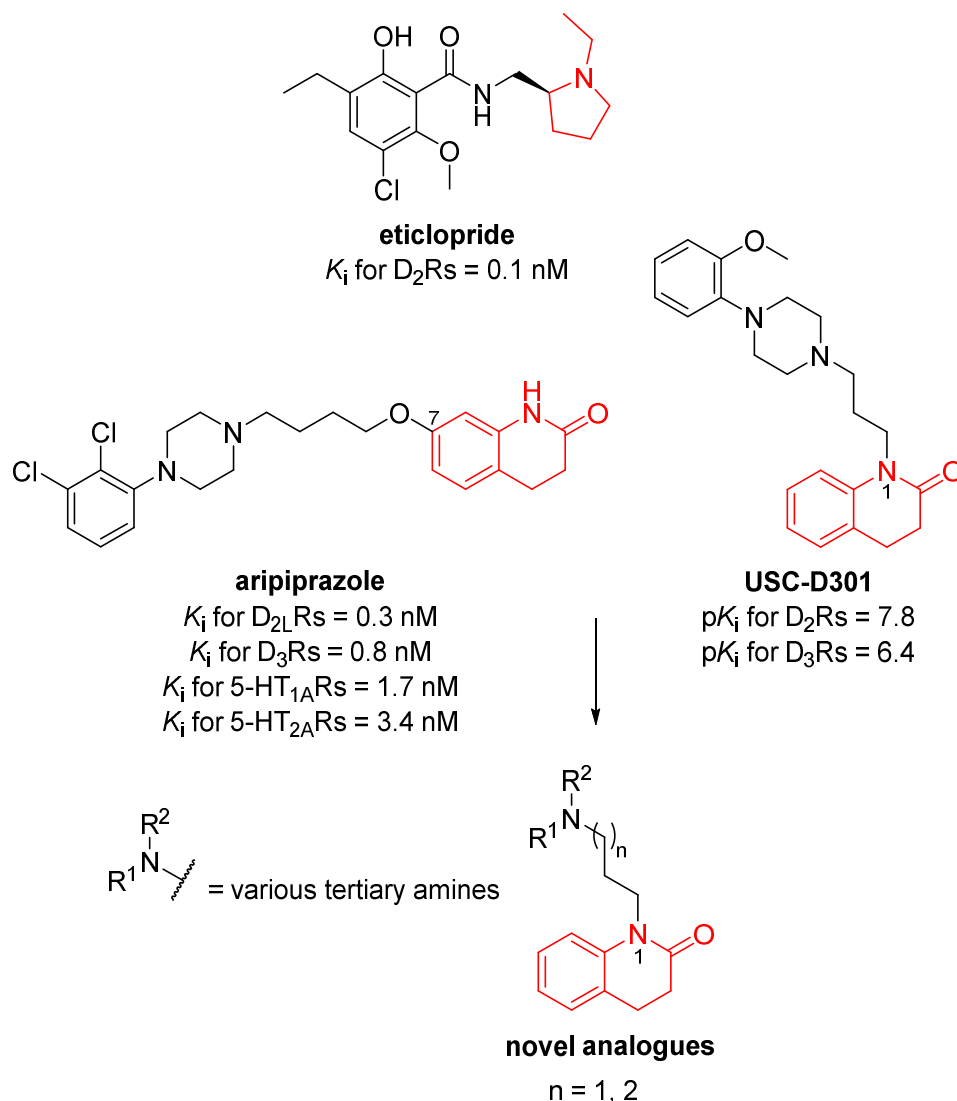


**Figure 1.** Design of novel 3,4-dihydroquinolin-2(1H)-one analogues from aripiprazole, eticlopride and USC-D301.

## 2. Materials and Methods

### 2.1. Chemistry

The chemicals were purchased from Sigma-Aldrich Co., LLC (Prague, Czech Republic) and were used without additional purification. Analytical thin-layer chromatography was carried out using plates coated with silica gel 60 with the fluorescent indicator F254 (Merck, Prague, Czech Republic). The thin-layer chromatography (TLC) plates were visualized by exposure to ultraviolet light (254 nm) or by the detection reagent ninhydrin. Column chromatography was performed using silica gel 100 at atmospheric pressure (70–230-mesh ASTM, Fluka, Prague, Czech Republic). The NMR spectra were all recorded on a Varian S500 spectrometer (500 MHz for  $^1H$  and 126 MHz for  $^{13}C$ ). Chemical shifts are reported in  $\delta$  ppm referenced to residual solvent signals (for  $^1H$  NMR and  $^{13}C$  NMR: chloroform-*d* ( $CDCl_3$ ; 7.26 (D) or 77.16 (C) ppm). A CEM Explorer SP 12 S was used for the MW-assisted reaction. The final compounds were analyzed by LC-MS with a Dionex Ultimate 3000 RS UHPLC system coupled with a Q Exactive Plus Orbitrap mass spectrometer (Thermo Fisher Scientific, Bremen, Germany) to obtain high-resolution mass spectra. Gradient LC analysis with UV detection (254 nm) confirmed >95% purity.

### 2.1.1. Preparation of 1-(3-chloropropyl)-3,4-dihydroquinolin-2(1H)-one (**4a**)

To a stirred solution of 3,4-dihydroquinolin-2-(1H)-one (**1**) (2.7 mmol) and 60% NaH (272 mg) in DMF (20 mL), 1-bromo-3-chloropropane (**2**) (3.0 mmol) was added in drop-by-drop manner under ice-cooled condition. After the addition of **2**, the reaction mixture was stirred for 4 h at room temperature (r.t.) [42]. After the completion of the reaction (monitored by TLC), the mixture was diluted with toluene (30 mL) and concentrated under reduced pressure. This operation was done three times. To the resulting mixture, DCM (200 mL) and distilled water (100 mL) were added, and it was vigorously stirred at r.t. for 30 min. The organic phase was then separated, dried over Na<sub>2</sub>SO<sub>4</sub>, filtered and concentrated under reduced pressure. The crude residue was purified by silica gel chromatography (DCM:EtOAc = 4:1 v/v).

The product was isolated as yellowish oil in 89% yield (540 mg); <sup>1</sup>H NMR of **4a** agrees with the literature-reported spectra [43]. <sup>1</sup>H NMR (500 MHz, CDCl<sub>3</sub>) δ 7.28–7.24 (m, 1H), 7.17 (dq, *J* = 7.4, 1.2 Hz, 1H), 7.07 (dd, *J* = 8.2, 1.1 Hz, 1H), 7.01 (td, *J* = 7.4, 1.1 Hz, 1H), 4.12–4.07 (m, 2H), 3.62 (t, *J* = 6.3 Hz, 2H), 2.89 (dd, *J* = 8.7, 6.1 Hz, 2H), 2.69–2.60 (m, 2H), 2.19–2.10 (m, 2H).

### 2.1.2. Preparation of 1-(4-chlorobutyl)-3,4-dihydroquinolin-2(1H)-one (**4b**)

To a stirred solution of 3,4-dihydroquinolin-2-(1H)-one (**1**) (6.1 mmol) and 60% NaH (624 mg) in DMF (18 mL), 1-bromo-4-chlorobutane (**3**) (12 mmol) was added in a drop-by-drop manner under ice-cooled condition. After the addition of **3**, the reaction mixture was stirred at r.t. overnight [42,44,45]. After the completion of the reaction (monitored by TLC), the mixture was diluted with toluene (30 mL) and concentrated under reduced pressure. This operation was done three times. To the resulting mixture, EtOAc (300 mL) and distilled water (100 mL) were added, and it was vigorously stirred at r.t. for 30 min. The organic phase was then separated, dried over Na<sub>2</sub>SO<sub>4</sub>, filtered and concentrated under reduced pressure. The crude residue was purified by silica gel chromatography (DCM:EtOAc = 98:2 v/v).

The product was isolated as yellowish oil in 70% yield (1.0 g); <sup>1</sup>H NMR (500 MHz, CDCl<sub>3</sub>) δ 7.27–7.23 (m, 1H), 7.20–7.14 (m, 1H), 7.01 (ddd, *J* = 8.5, 5.8, 1.2 Hz, 2H), 3.98 (t, *J* = 7.0 Hz, 2H), 3.58 (t, *J* = 6.1 Hz, 2H), 2.89 (dd, *J* = 8.7, 6.1 Hz, 2H), 2.67–2.58 (m, 2H), 1.82 (tdd, *J* = 9.0, 7.4, 4.9 Hz, 4H). <sup>13</sup>C NMR (126 MHz, CDCl<sub>3</sub>) δ 170.4, 139.4, 128.2, 127.6, 126.7, 122.9, 114.8, 44.7, 41.2, 32.0, 29.9, 25.7, 24.7.

### 2.1.3. General Procedure for the Preparation of Final Compounds **5a-g** and **6a-g**

To a stirred solution of appropriate analogue **4a,b** (0.5 mmol) and amine **a-g** (1.5 mmol) in MeCN (5 mL), K<sub>2</sub>CO<sub>3</sub> (1.5 mmol) was added and the reaction mixture was stirred for overnight at reflux [46]. After the completion of the reaction (monitored by TLC), the mixture was diluted with CHCl<sub>3</sub> (30 mL), the solid was filtered off and the residue was concentrated under reduced pressure. The crude product was purified by silica gel chromatography (DCM:MeOH = 95:5 v/v). Final compounds (**5a-g**, **6a-g**) were prepared as hydrochlorides by mixing with small portion of hydrochloric acid (37% aq.) in MeOH at r.t.

1-(3-(Pyrrolidin-1-yl)propyl)-3,4-dihydroquinolin-2(1H)-one (**5a**), Colorless oil. Yield: 56% (72 mg); <sup>1</sup>H NMR (500 MHz, CDCl<sub>3</sub>) δ 7.21 (td, *J* = 7.8, 1.6 Hz, 1H), 7.13 (dd, *J* = 7.5, 1.5 Hz, 1H), 7.05 (d, *J* = 8.1 Hz, 1H), 6.97 (t, *J* = 7.3 Hz, 1H), 4.01–3.95 (m, 2H), 2.86 (dd, *J* = 8.7, 6.1 Hz, 2H), 2.65–2.53 (m, 8H), 1.90 (p, *J* = 7.5 Hz, 2H), 1.79 (h, *J* = 3.1 Hz, 4H). <sup>13</sup>C NMR (126 MHz, CDCl<sub>3</sub>) δ 170.3, 139.6, 128.1, 127.6, 126.6, 122.8, 115.0, 54.2, 53.7, 40.6, 32.0, 26.6, 25.6, 23.5. LC-MS: calc *m/z* = 259.180232 for C<sub>16</sub>H<sub>23</sub>N<sub>2</sub>O<sup>+</sup>; found [M+H]<sup>+</sup> = 259.1802; 99% purity.

1-(3-(Piperidin-1-yl)propyl)-3,4-dihydroquinolin-2(1H)-one (**5b**), Colorless oil. Yield: 64% (87 mg); <sup>1</sup>H NMR (500 MHz, CDCl<sub>3</sub>) δ 7.24–7.19 (m, 1H), 7.14 (d, *J* = 7.3 Hz, 1H), 7.08 (d, *J* = 8.2 Hz, 1H), 6.98 (t, *J* = 7.4 Hz, 1H), 3.96 (t, *J* = 7.5 Hz, 2H), 2.87 (dd, *J* = 8.7, 6.1 Hz, 2H), 2.62 (dd, *J* = 8.7, 6.1 Hz, 2H), 2.45–2.39 (m, 6H), 1.87 (p, *J* = 7.5 Hz, 2H), 1.61 (p, *J* = 5.7 Hz, 4H), 1.43 (p, *J* = 5.9 Hz, 2H). <sup>13</sup>C NMR (126 MHz, CDCl<sub>3</sub>) δ 170.3, 139.7, 128.0, 127.6, 126.6,

122.8, 115.1, 56.4, 54.6, 40.6, 32.0, 25.8, 25.7, 24.6, 24.3. LC-MS: calc  $m/z = 273.1961$  for  $C_{17}H_{25}N_2O^+$ ; found  $[M+H]^+ = 273.1945$ ; 98% purity.

*1-(3-(4-Methylpiperazin-1-yl)propyl)-3,4-dihydroquinolin-2(1H)-one (5c)*, Yellowish oil. Yield: 51% (72 mg);  $^1H$  NMR (500 MHz,  $CDCl_3$ )  $\delta$  7.21 (td,  $J = 7.8, 1.6$  Hz, 1H), 7.14 (dd,  $J = 7.4, 1.5$  Hz, 1H), 7.06 (dd,  $J = 8.2, 1.0$  Hz, 1H), 6.98 (td,  $J = 7.4, 1.1$  Hz, 1H), 4.04–3.89 (m, 2H), 2.87 (dd,  $J = 8.7, 6.1$  Hz, 2H), 2.66–2.57 (m, 2H), 2.50 (s, 8H), 2.42 (t,  $J = 7.2$  Hz, 2H), 2.30 (s, 3H), 1.82 (p,  $J = 7.2$  Hz, 2H).  $^{13}C$  NMR (126 MHz,  $CDCl_3$ )  $\delta$  170.3, 139.7, 128.1, 127.5, 126.6, 122.8, 115.0, 55.6, 55.1, 53.0, 45.9, 40.5, 32.0, 25.7, 24.8. LC-MS: calc  $m/z = 288.2070$  for  $C_{17}H_{26}N_3O^+$ ; found  $[M+H]^+ = 288.2065$ ; 98% purity.

*1-(3-Morpholinopropyl)-3,4-dihydroquinolin-2(1H)-one (5d)*, Yellowish oil. Yield: 45% (62 mg);  $^1H$  NMR (500 MHz,  $CDCl_3$ )  $\delta$  7.21 (td,  $J = 7.8, 1.6$  Hz, 1H), 7.14 (dd,  $J = 7.4, 1.5$  Hz, 1H), 7.06 (d,  $J = 7.9$  Hz, 1H), 6.98 (td,  $J = 7.4, 1.1$  Hz, 1H), 4.01–3.95 (m, 2H), 3.70 (t,  $J = 4.7$  Hz, 4H), 2.87 (dd,  $J = 8.7, 6.1$  Hz, 2H), 2.67–2.59 (m, 2H), 2.48–2.36 (m, 6H), 1.83 (p,  $J = 7.3$  Hz, 2H).  $^{13}C$  NMR (126 MHz,  $CDCl_3$ )  $\delta$  170.3, 139.7, 128.1, 127.5, 126.6, 122.8, 114.9, 67.0, 56.2, 53.8, 40.5, 32.0, 25.7, 24.4. LC-MS: calc  $m/z = 275.1754$  for  $C_{16}H_{23}N_2O_2^+$ ; found  $[M+H]^+ = 275.1749$ ; 95% purity.

*1-(3-Thiomorpholinopropyl)-3,4-dihydroquinolin-2(1H)-one (5e)*, Colorless oil. Yield: 47% (68 mg);  $^1H$  NMR (500 MHz,  $CDCl_3$ )  $\delta$  7.23 (td,  $J = 7.9, 1.6$  Hz, 1H), 7.15 (dd,  $J = 7.5, 1.4$  Hz, 1H), 7.05 (d,  $J = 8.1$  Hz, 1H), 6.99 (t,  $J = 7.4$  Hz, 1H), 3.99–3.93 (m, 2H), 2.88 (dd,  $J = 8.7, 6.1$  Hz, 2H), 2.76–2.66 (m, 8H), 2.66–2.59 (m, 2H), 2.45 (t,  $J = 7.2$  Hz, 2H), 1.83 (p,  $J = 7.2$  Hz, 2H).  $^{13}C$  NMR (126 MHz,  $CDCl_3$ )  $\delta$  170.3, 139.7, 128.1, 127.5, 126.6, 122.9, 114.9, 56.4, 55.1, 40.5, 32.0, 27.9, 25.7, 24.3. LC-MS: calc  $m/z = 291.1526$  for  $C_{16}H_{23}N_2OS^+$ ; found  $[M+H]^+ = 291.1520$ ; 95% purity.

*1-(3-(Diethylamino)propyl)-3,4-dihydroquinolin-2(1H)-one (5f)*, Colorless oil. Yield: 45% (59 mg);  $^1H$  NMR (500 MHz,  $CDCl_3$ )  $\delta$  7.23 (td,  $J = 7.8, 1.6$  Hz, 1H), 7.17–7.12 (m, 1H), 7.06 (d,  $J = 8.1$  Hz, 1H), 6.99 (t,  $J = 7.4$  Hz, 1H), 4.00–3.93 (m, 2H), 2.87 (dd,  $J = 8.7, 6.1$  Hz, 2H), 2.66–2.54 (m, 8H), 1.89–1.80 (m, 2H), 1.09–1.02 (m, 6H).  $^{13}C$  NMR (126 MHz,  $CDCl_3$ )  $\delta$  170.4, 139.6, 128.1, 127.6, 126.6, 122.9, 115.0, 50.3, 46.9, 40.7, 32.0, 25.7, 24.6, 11.4. LC-MS: calc  $m/z = 261.1961$  for  $C_{16}H_{25}N_2O^+$ ; found  $[M+H]^+ = 261.1958$ ; 98% purity.

*1-(3-((2-Methoxyethyl)(methyl)amino)propyl)-3,4-dihydroquinolin-2(1H)-one (5g)*, Yellowish oil. Yield: 52% (72 mg);  $^1H$  NMR (500 MHz,  $CDCl_3$ )  $\delta$  7.25–7.20 (m, 1H), 7.17–7.12 (m, 1H), 7.06 (d,  $J = 8.1$  Hz, 1H), 6.98 (tt,  $J = 7.4, 1.0$  Hz, 1H), 3.99–3.93 (m, 2H), 3.49 (td,  $J = 5.7, 1.2$  Hz, 2H), 3.34 (d,  $J = 0.7$  Hz, 3H), 2.87 (dd,  $J = 8.7, 6.1$  Hz, 2H), 2.65–2.57 (m, 4H), 2.55–2.48 (m, 2H), 2.30 (d,  $J = 1.4$  Hz, 3H), 1.88–1.80 (m, 2H).  $^{13}C$  NMR (126 MHz,  $CDCl_3$ )  $\delta$  170.3, 139.7, 128.1, 127.6, 126.6, 122.8, 115.0, 70.5, 59.0, 56.7, 55.5, 42.7, 40.6, 32.0, 25.7, 24.9. LC-MS: Calc  $m/z = 277.1911$  for  $C_{16}H_{25}N_2O_2^+$ ; found  $[M+H]^+ = 277.1910$ ; 98% purity.

*1-(4-(Pyrrolidin-1-yl)butyl)-3,4-dihydroquinolin-2(1H)-one (6a)*, Colorless oil. Yield: 59% (71 mg);  $^1H$  NMR (500 MHz,  $CDCl_3$ )  $\delta$  7.25–7.18 (m, 1H), 7.14 (d,  $J = 7.3$  Hz, 1H), 7.02–6.95 (m, 2H), 3.93 (d,  $J = 6.7$  Hz, 2H), 2.90–2.83 (m, 2H), 2.74 (dt,  $J = 7.2, 3.6$  Hz, 4H), 2.69–2.64 (m, 2H), 2.64–2.58 (m, 2H), 1.87 (h,  $J = 2.7$  Hz, 4H), 1.69 (dq,  $J = 5.9, 3.4$  Hz, 4H).  $^{13}C$  NMR (126 MHz,  $CDCl_3$ )  $\delta$  170.4, 139.4, 128.1, 127.6, 126.6, 122.9, 114.9, 55.7, 54.0, 41.5, 32.0, 25.6, 25.1, 25.0, 23.5. LC-MS: Calc  $m/z = 273.1961$  for  $C_{17}H_{25}N_2O^+$ ; found  $[M+H]^+ = 273.1957$ ; 99% purity.

*1-(4-(Piperidin-1-yl)butyl)-3,4-dihydroquinolin-2(1H)-one (6b)*, Colorless oil. Yield: 61% (87 mg);  $^1H$  NMR (500 MHz,  $CDCl_3$ )  $\delta$  7.29–7.24 (m, 1H), 7.18 (d,  $J = 7.3$  Hz, 1H), 7.08 (d,  $J = 8.1$  Hz, 1H), 7.02 (t,  $J = 7.4$  Hz, 1H), 4.00–3.94 (m, 2H), 2.90 (dd,  $J = 8.7, 6.2$  Hz, 2H), 2.65 (dd,  $J = 8.8, 6.1$  Hz, 2H), 2.44 (dd,  $J = 17.9, 10.2$  Hz, 6H), 1.67 (qt,  $J = 12.0, 4.9$  Hz, 8H), 1.48 (p,  $J = 5.9$  Hz, 2H).  $^{13}C$  NMR (126 MHz,  $CDCl_3$ )  $\delta$  170.3, 139.6, 128.1, 127.5, 126.6, 122.8, 115.0, 58.6, 54.5, 41.9, 32.0, 25.7, 25.1, 24.3, 23.8. LC-MS: Calc  $m/z = 287.2118$  for  $C_{18}H_{27}N_2O^+$ ; found  $[M+H]^+ = 287.2118$ ; 97% purity.

*1-(4-(4-Methylpiperazin-1-yl)butyl)-3,4-dihydroquinolin-2(1H)-one (6c)*, Yellowish oil. Yield: 69% (104 mg);  $^1H$  NMR (500 MHz,  $CDCl_3$ )  $\delta$  7.22 (td,  $J = 7.8, 1.6$  Hz, 1H), 7.13 (dd,  $J = 7.4, 1.5$  Hz, 1H), 7.05–7.00 (m, 1H), 6.97 (td,  $J = 7.4, 1.1$  Hz, 1H), 3.92 (dd,  $J = 8.7, 6.5$  Hz, 2H), 2.86 (dd,  $J = 8.7, 6.1$  Hz, 2H), 2.64–2.57 (m, 2H), 2.53–2.46 (m, 8H), 2.42–2.35 (m, 2H), 2.29 (s,



3H), 1.65 (ddd,  $J = 15.1, 9.0, 7.0$  Hz, 2H), 1.60–1.51 (m, 2H).  $^{13}\text{C}$  NMR (126 MHz,  $\text{CDCl}_3$ )  $\delta$  170.2, 139.6, 128.1, 127.5, 126.6, 122.8, 115.0, 57.8, 55.0, 52.9, 45.9, 41.9, 32.0, 25.6, 25.0, 24.0. LC-MS: calc  $m/z = 302.2227$  for  $\text{C}_{18}\text{H}_{28}\text{N}_3\text{O}^+$ ; found  $[\text{M}+\text{H}]^+ = 302.2228$ ; 98% purity.

*1-(4-Morpholinobutyl)-3,4-dihydroquinolin-2(1H)-one (6d)*, Yellowish oil. Yield: 64% (92 mg);  $^1\text{H}$  NMR (500 MHz,  $\text{CDCl}_3$ )  $\delta$  7.23 (td,  $J = 7.8, 1.6$  Hz, 1H), 7.15 (dd,  $J = 7.5, 1.5$  Hz, 1H), 7.03 (d,  $J = 8.2$  Hz, 1H), 6.99 (t,  $J = 7.4$  Hz, 1H), 3.98–3.91 (m, 2H), 3.73 (t,  $J = 4.8$  Hz, 4H), 2.87 (dd,  $J = 8.7, 6.1$  Hz, 2H), 2.62 (dd,  $J = 8.7, 6.1$  Hz, 2H), 2.49–2.44 (m, 4H), 2.41 (t,  $J = 7.4$  Hz, 2H), 1.73–1.63 (m, 2H), 1.63–1.55 (m, 2H).  $^{13}\text{C}$  NMR (126 MHz,  $\text{CDCl}_3$ )  $\delta$  170.3, 139.6, 128.1, 127.5, 126.7, 122.9, 115.0, 66.8, 58.3, 53.6, 41.8, 32.0, 25.7, 24.9, 23.5. LC-MS: calc  $m/z = 288.1838$  for  $\text{C}_{17}\text{H}_{24}\text{N}_2\text{O}_2$ ; found  $[\text{M}+\text{H}]^+ = 289.1911$ ; 96% purity.

*1-(4-Thiomorpholinobutyl)-3,4-dihydroquinolin-2(1H)-one (6e)*, Colorless oil. Yield: 58% (88 mg);  $^1\text{H}$  NMR (500 MHz,  $\text{CDCl}_3$ )  $\delta$  7.23 (td,  $J = 7.9, 1.6$  Hz, 1H), 7.15 (dd,  $J = 7.5, 1.5$  Hz, 1H), 7.03 (d,  $J = 8.2$  Hz, 1H), 6.99 (t,  $J = 7.4$  Hz, 1H), 3.97–3.90 (m, 2H), 2.87 (dd,  $J = 8.7, 6.1$  Hz, 2H), 2.76–2.65 (m, 8H), 2.65–2.59 (m, 2H), 2.41 (t,  $J = 7.3$  Hz, 2H), 1.65 (ddd,  $J = 15.1, 8.8, 6.8$  Hz, 2H), 1.56 (ddd,  $J = 14.8, 8.3, 6.0$  Hz, 2H).  $^{13}\text{C}$  NMR (126 MHz,  $\text{CDCl}_3$ )  $\delta$  170.3, 139.6, 128.1, 127.5, 126.7, 122.8, 115.0, 58.6, 55.0, 41.9, 32.0, 28.0, 25.7, 25.0, 23.6. LC-MS: Calc  $m/z = 305.1682$  for  $\text{C}_{17}\text{H}_{25}\text{N}_2\text{OS}^+$ ; found  $[\text{M}+\text{H}]^+ = 305.1683$ ; 95% purity.

*1-(4-(Diethylamino)butyl)-3,4-dihydroquinolin-2(1H)-one (6f)*, Yellowish oil. Yield: 49% (67 mg);  $^1\text{H}$  NMR (500 MHz,  $\text{CDCl}_3$ )  $\delta$  7.23 (td,  $J = 7.8, 1.6$  Hz, 1H), 7.15 (dd,  $J = 7.4, 1.5$  Hz, 1H), 7.03 (d,  $J = 8.2$  Hz, 1H), 6.99 (td,  $J = 7.4, 1.1$  Hz, 1H), 3.97–3.91 (m, 2H), 2.87 (dd,  $J = 8.7, 6.1$  Hz, 2H), 2.67–2.55 (m, 6H), 2.55–2.50 (m, 2H), 1.66 (ddd,  $J = 14.9, 8.9, 6.9$  Hz, 2H), 1.61–1.54 (m, 2H), 1.06 (t,  $J = 7.2$  Hz, 6H).  $^{13}\text{C}$  NMR (126 MHz,  $\text{CDCl}_3$ )  $\delta$  170.3, 139.6, 128.1, 127.6, 126.7, 122.8, 115.0, 52.3, 46.8, 41.9, 32.0, 25.7, 25.2, 24.0, 11.3. LC-MS: Calc  $m/z = 275.2118$  for  $\text{C}_{17}\text{H}_{27}\text{N}_2\text{O}^+$ ; found  $[\text{M}+\text{H}]^+ = 275.2119$ ; 96% purity.

*1-(4-((2-Methoxyethyl)(methyl)amino)butyl)-3,4-dihydroquinolin-2(1H)-one (6g)*, Yellowish oil. Yield: 59% (86 mg);  $^1\text{H}$  NMR (500 MHz,  $\text{CDCl}_3$ )  $\delta$  7.23 (td,  $J = 7.8, 1.6$  Hz, 1H), 7.14 (dd,  $J = 7.4, 1.5$  Hz, 1H), 7.03–6.94 (m, 2H), 3.97–3.90 (m, 2H), 3.48 (td,  $J = 5.7, 1.0$  Hz, 2H), 3.33 (s, 3H), 2.87 (dd,  $J = 8.7, 6.1$  Hz, 2H), 2.65–2.55 (m, 4H), 2.48–2.41 (m, 2H), 2.28 (d,  $J = 1.1$  Hz, 3H), 1.73–1.61 (m, 2H), 1.56 (ddd,  $J = 15.3, 8.5, 5.9$  Hz, 2H).  $^{13}\text{C}$  NMR (126 MHz,  $\text{CDCl}_3$ )  $\delta$  170.3, 139.6, 128.1, 127.5, 126.7, 122.8, 115.0, 70.6, 59.0, 57.7, 56.8, 42.6, 42.0, 32.0, 25.7, 25.1, 24.4. LC-MS: Calc  $m/z = 291.2067$  for  $\text{C}_{17}\text{H}_{27}\text{N}_2\text{O}_2^+$ ; found  $[\text{M}+\text{H}]^+ = 291.2068$ ; 99% purity.

## 2.2. Molecular Studies

### 2.2.1. Docking Simulation

Molecular docking of ligands was performed using the Molecular Operating Environment (MOE) software package [47]. The receptor used was pdb structure 6CM4, which contains a structure of the atypical antipsychotic drug and  $\text{D}_2\text{R}$  antagonist risperidone bound to the  $\text{D}_2\text{R}$  [48]. An induced fit docking protocol was used, with the Triangle Matcher used for placement (10,000 placements), London dG scoring function used for initial scoring (100 conformations retained), refinement with Amber10:EHT force field, and rescoring with GBVI/WSA dG (100 conformations retained and ranked by docking score). Before docking, compounds were prepared by protonation at physiological pH and energy minimization with Amber10:EHT force field.

### 2.2.2. Thermodynamic Integration and Free Energy Calculations

Final docked conformations of risperidone, aripiprazole, USC-D301, and **5e** were generated using the preceding method. For thermodynamic integration standard settings were used (Figure S60, Supplementary Material). The used force field was Amber10:EHT. Preparation of the molecular system was done using MOE, the thermodynamic free energy calculation was performed using the PMEMD package of the AMBER molecular dynamics toolkit [47].

### 2.3. BBB Score Prediction

Blood–brain barrier (BBB) score of newly developed compounds was calculated using an algorithm defined by Gupta et al. [49]. A MarvinSketch software (ChemAxon Ltd., v. 20.15.0; <https://www.chemaxon.com>) was used to predict some of the physicochemical descriptors like number of aromatic ring, number heavy atoms, MWHBN (a descriptor comprising molecular weight, hydrogen bond donor, and hydrogen bond acceptors), topological polar surface area, and  $pK_A$ .

### 2.4. Biology Evaluation

#### 2.4.1. D2 Receptor Binding Affinity–Transfection and Membrane Preparation

Chinese hamster ovary cells (CHO cells) were used for the binding experiments. About 24 h before transfection, CHO cells were plated on a 10 cm Petri dish at a density of  $1.5 \times 10^6$  cells and cultivated in 10 mL DMEM/Ham's F12 supplemented with 10% heat-inactivated fetal bovine serum (FBS).

For transfection, the desired amount of linear polyethyleneimine (PEI) 25\_K (Polysciences, Eppelheim, Germany) and DNA (dopamine receptor (D2) wild type, cDNA resource centre, Bloomsberg, PA, USA) were diluted separately in phosphate buffer saline (PBS). After 20 min, DNA was added to PEI solution, mixed and left for an additional 30 min. Final concentration of reactants was 6  $\mu$ g plasmid DNA and 18  $\mu$ g PEI per mL. PEI/DNA complex was added (1 mL/dish) and the plates were incubated for another 24 h. Then, the medium was replaced with fresh DMEM/Ham's F12 with 10% FBS and incubated for an additional 24 h. Cells were maintained at 37 °C in a 5% CO<sub>2</sub> humidified atmosphere.

About 48 h after transfection, cells were washed with PBS, mechanically detached from the dish with a plastic scraper in the ice-cold PBS, and centrifuged for 3 min at  $250 \times g$ . Pellet was suspended in the ice-cold homogenization medium (100 mM NaCl, 20 mM Na-HEPES, 10 mM EDTA, pH 7.4) and homogenized on ice by two 30-s strokes using Polytron homogenizer (Ultra-Turrax; Janke & Kunkel GmbH & Co. KG, IKA-Labortechnik, Staufen, Germany) with a 30-s pause between strokes. Cell homogenates were centrifuged for 5 min at  $1000 \times g$ . The supernatant was collected and centrifuged for 30 min at  $30,000 \times g$ . Pellets were suspended in incubation medium (100 mM NaCl, 20 mM Na-HEPES, 10 mM MgCl<sub>2</sub>, pH 7.4), left for 30 min at 4 °C and centrifuged again for 30 min at  $30,000 \times g$ . The membrane pellets were kept at  $-80$  °C until use.

#### 2.4.2. D<sub>2</sub>R Binding Affinity–Radioligand Experiment

All radioligand binding experiments were optimized and carried out as described by El-Fakahany and Jakubik [50]. Dissociation constant  $K_D$  of [<sup>3</sup>H]-spiperone to D<sub>2</sub>Rs was determined in saturation binding experiment. Saturation experiments were performed in 800  $\mu$ L volume containing: 400  $\mu$ L of the membrane suspension and 400  $\mu$ L of the radioligand in six increasing concentrations (ranging from 31 to 1000 pM).

Affinity of the tested compounds was determined in competition experiments with 180 pM [<sup>3</sup>H]-spiperone, that corresponds to triple  $K_D$  value ([<sup>3</sup>H]-spiperone,  $K_d = 60.1 \pm 2.79$  pM ( $n = 6$ )). The examined compounds were diluted in incubation buffer and tested in six concentrations (ranging from 0.1 nM–1 mM). The reactions were performed in 400  $\mu$ L volume containing: 100  $\mu$ L of the radioligand, 100  $\mu$ L of tested substances dilution, and 200  $\mu$ L of the membranes.

Nonspecific binding was determined in the presence of 10  $\mu$ M unlabeled sulpiride. Membrane suspensions from both saturation and binding experiments (approximately 10  $\mu$ g of membrane proteins per sample) were incubated in 96-well plates for 1 h at 25 °C in the incubation medium (100 mM NaCl, 20 mM Na-HEPES, 10 mM MgCl<sub>2</sub>, pH = 7.4) in a shaking incubator (25 °C; PST-60HL, Biosan, Riga, Latvia).

The binding reactions were terminated by filtration of the membranes through APFC filter plate (Millipore, Prague, Czech Republic) pre-soaked with 0.5% PEI and washed with ice-cold distilled water using a Brandel cell harvester (Brandel, Gaithersburg, MD, USA). Then, filters with labelled membranes were dried. After 24 h, scintillation cocktail

(Rotiszint eco plus, Carl Roth) was added to each sample and radioactivity was quantified by liquid scintillation spectrometry using Wallac Microbeta scintillation counter (Wallac, Turku, Finland). Competition binding experiments were performed per triplicate and all experiments were performed three times. Protein concentration was determined by the Lowry method in the Peterson modification [51].

#### 2.4.3. D2 Receptor Binding Affinity–Data Analysis

##### [<sup>3</sup>H]NMS Saturation Binding

The equilibrium dissociation constant ( $K_D$ ) and maximum binding capacity ( $B_{MAX}$ ) were determined in the saturation experiments. Non-specific binding in the presence of 10  $\mu$ M sulpiride was subtracted to determine specific binding. Free concentration of [<sup>3</sup>H]-spiperone was calculated by subtraction of values of specific binding from the final concentration of [<sup>3</sup>H]-spiperone calculated from measurements of added radioactivity. Equation (1) was fitted to the data.

$$y = \frac{B_{MAX} * x}{K_D + x} \quad (1)$$

where  $y$  is the specific binding at free concentration  $x$ .  $K_D$  values are expressed as  $\mu$ M and  $B_{MAX}$  values as pmol of binding sites per mg of membrane protein.

##### Competition Binding

The binding of tested agonists was determined in competition experiments with 180 pM [<sup>3</sup>H]-Spiperone fitting of Equation (2)

$$y = 100 - \frac{100 * x}{x + IC_{50}} \quad (2)$$

where  $y$  is the specific radioligand binding at concentration  $x$  of competitor expressed as a percent of binding in the absence of a competitor,  $IC_{50}$  is the concentration causing 50% inhibition of radioligand binding. Inhibition constants  $K_I$  for analyzed agonists were calculated as:

$$K_I = \frac{IC_{50}}{1 + \frac{[D]}{K_D}} \quad (3)$$

where  $IC_{50}$  is the concentration causing 50% inhibition of [<sup>3</sup>H]-spiperone binding calculated according to Equation (2) from competition binding data,  $[D]$  is the concentration of [<sup>3</sup>H]NMS used, and  $K_D$  is its equilibrium dissociation constant calculated according to Equation (1) from saturation binding data.

#### 2.4.4. MTT Assay

Standard MTT (3-[4,5-dimethylthiazol-2-yl]-2,5-diphenyltetrazolium bromide) assay (Sigma Aldrich, Prague, Czech Republic) was used according to the manufacturer's protocol on the CHO-K1 (Chinese hamster ovary, ECACC, Salisbury, UK) in order to compare the effect of different compounds within the series. The cells were cultured according to ECACC recommended conditions and seeded in a density of 8000 per well as described previously [52]. Briefly, tested compounds were dissolved in DMSO (Sigma Aldrich, Prague, Czech Republic) and subsequently in the growth medium (F-12) so that the final concentration of DMSO did not exceed 1% ( $v/v$ ). Cells were exposed to a tested compound for 24 h. Then the medium was replaced by a medium containing 10  $\mu$ M of MTT and cells were allowed to produce formazan for another approximately 3 h under surveillance. Thereafter, medium with MTT was sucked out and crystals of formazan were dissolved in DMSO (100  $\mu$ L). Cell viability was assessed spectrophotometrically by the amount of formazan produced. Absorbance was measured at 570 nm with 650 nm reference wavelength on Synergy HT (BioTek, Winooski, VT, USA).  $IC_{50}$  was then calculated from the control-subtracted



triplicates using non-linear regression (four parameters) of GraphPad Prism 9 software. Final  $IC_{50}$  and SEM values were obtained as a mean of three independent measurements.

#### 2.4.5. PAMPA Assay

PAMPA is a high-throughput screening tool applicable for prediction of the passive transport of potential drugs across the BBB [53]. In this study, it has been used as a non-cell-based in vitro assay carried out in a coated 96-well membrane filter. The filter membrane of the donor plate was coated with PBL (Polar Brain Lipid, Avanti, AL, USA) in dodecane (4  $\mu$ L of 20 mg/mL PBL in dodecane) and the acceptor well was filled with 300  $\mu$ L of PBS pH 7.4 buffer ( $V_A$  tested compounds were dissolved first in the DMSO/phosphate-buffered saline mixture (maximum 0.5% *v/v* of DMSO) and subsequently diluted with phosphate-buffered saline (pH 7.4) to final concentrations of 40–100  $\mu$ M in the donor wells). Concentration of DMSO did not exceed 0.5% (*v/v*) in the donor solution. About 300  $\mu$ L of the donor solution was added to the donor wells ( $V_D$ ) and the donor filter plate was carefully put on the acceptor plate so that coated membrane was “in touch” with both donor solution and acceptor buffer. Test compound diffused from the donor well through the lipid membrane (Area = 0.28 cm<sup>2</sup>) to the acceptor well. The concentration of the drug in both donor and the acceptor wells were assessed after 3, 4, 5, and 6 h of incubation in quadruplicate using the UV plate reader Synergy HT (Biotek, Winooski, VT, USA) at the maximum absorption wavelength of each compound. Besides that, solution of theoretical compound concentration, simulating the equilibrium state established if the membrane were ideally permeable was prepared and assessed as well. Concentration of the compounds in the donor and acceptor well and equilibrium concentration were calculated from the standard curve and expressed as the permeability ( $P_e$ ) according to the equation:

$$P_e = C \times \ln \left( 1 - \frac{[drug]_{acceptor}}{[drug]_{equilibrium}} \right) \text{ where } C = \frac{(V_D \times V_A)}{(V_D \times V_A) \text{ Area} \times \text{Time}} \quad (4)$$

### 3. Results

#### 3.1. Design of Novel Compounds

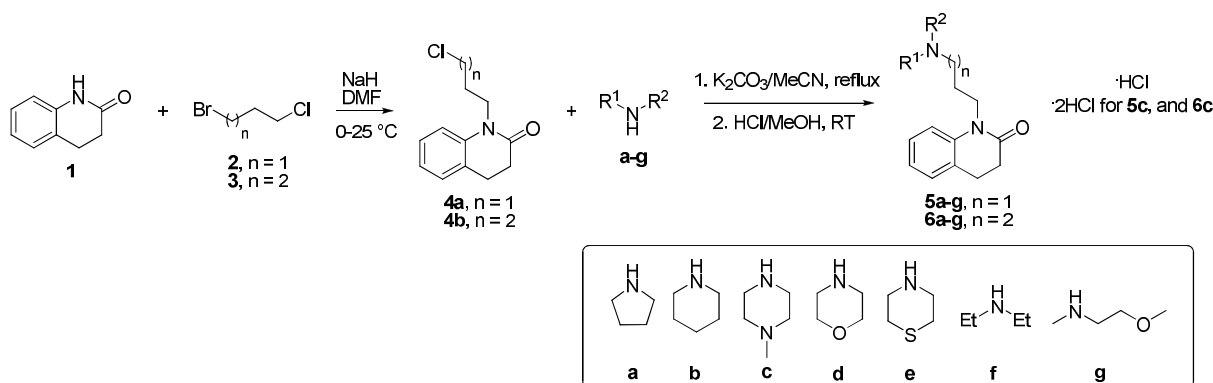
Aripiprazole (Figure 1), a partial D<sub>2</sub>Rs agonist, belongs to the third generation of antipsychotic drugs and has been approved by the Food and Drug Administration (FDA) agency for the use as an adjunctive medication in the treatment of depressive and bipolar disorders [9,11,54–56]. Aripiprazole has a unique, biased, mode of action comprising partial agonism for G $\alpha_{i/o}$  and a robust antagonism for G $\beta\gamma$  signaling and an antagonism or a partial agonism for  $\beta$ -arrestin-2 signaling [57,58]. Furthermore, if extracellular concentration of dopamine levels are high (e.g., in mesolimbic areas), aripiprazole competes with dopamine and acts as a partial antagonist. On the other hand, in the presence of low dopamine concentration (e.g., dopamine areas that are involved in working memory), aripiprazole can activate other receptors. Thus, aripiprazole can be classified as a “dopamine stabilizer” [9,59,60]. In addition, aripiprazole is a D<sub>3</sub> and 5-HT<sub>1A</sub> receptors partial agonist and 5-HT<sub>2A</sub>Rs antagonist [54,61]. In its structure, aripiprazole combines 3,4-dihydro-7-hydroxyquinolin-2(1H)-one fragment attached at position 7- to 2,3-dichlorophenyl piperazine and thus is a member of large group of antipsychotics, so called 1,4-disubstituted arylpiperazines. The biological activity of this subgroup of compounds is encoded by an aromatic warhead, which controls intrinsic activity, and an amine moiety, which is responsible for the formation of a hydrogen bond to the crucial residue Asp<sup>3.32</sup> in the transmembrane helix 3 of D<sub>2</sub>R [62]. A linker controls subtype selectivity; 3-methylene linker was found suitable for D<sub>2</sub>R selectivity [63,64]. Aromatic/heteroaromatic appendage on the opposite site of the ligand orchestrates receptor affinity [62]. In the past decade, many compounds have been generated containing 2,3-dichlorophenylpiperazine fragment with unique pharmacological profile exhibiting high D<sub>2</sub>Rs affinity. From the extensive SAR, it was deduced that the central linker has only moderate impact on affinity but huge effect

on functional activity at D<sub>2</sub>Rs [65–68]. Besides various substitutions made to the central linker, it has been shown that lipophilic appendages strongly influence functional and subtype selectivity [68–70]. 3,4-Dihydroquinolin-2(1*H*)-one scaffold-containing ligands have shown to possess an affinity to D<sub>2</sub>Rs as well. In this case, the nature of the central linker showed a moderate impact on D<sub>2</sub>Rs affinity [71]. Modifications within the amine moiety influenced D<sub>2</sub>Rs affinity and functional selectivity [72]. Besides, substitutions in aromatic warheads also strongly affected D<sub>2</sub>Rs affinity and functional and subtype selectivity [71,72]. Recently, some 3,4-dihydroquinolin-2-(1*H*)-one scaffold-containing compounds exhibited high D<sub>4</sub>Rs selectivity over other D<sub>2</sub>-like family receptors [73]. These findings show that small structural modifications within one region of the molecule based on aripiprazole can tune significantly the properties of the ligand.

In the study of López et al., researchers tethered arylpiperazine-like core (different phenylpiperazine moieties) with 3,4-dihydroquinolin-2(1*H*)-one moiety (red color, Figure 1) at position 1- [41]. USC-D301 (Figure 1) is an example of small molecule exhibiting strong D<sub>2</sub>R antagonism and high selectivity over D<sub>3</sub>Rs [41]. On the other hand, eticlopride (Figure 1) is a substituted benzamide analog without 1,4-disubstituted arylpiperazine fragment exhibiting very high affinity for D<sub>2</sub>Rs [74]. Thus, we wanted to explore the effect of novel prepared analogs containing various tertiary amines with 3,4-dihydroquinolin-2(1*H*)-one fragment connected by aliphatic linker at position 1- of the quinolinone core towards the D<sub>2</sub>Rs as the main targets. We are aware of the fact that other dopamine receptors (especially D<sub>3</sub>R and D<sub>4</sub>R) are of importance for the complexity of the antipsychotic action, as observed also in case of aripiprazole [54], however, this was not the aim of this study. Molecular imaging studies have revealed that striatal D<sub>2</sub>Rs antagonism is essential in vivo for therapeutic doses of all neuroleptics [19,75–80], and D<sub>2</sub>Rs affinity of antipsychotic drugs is the crucial for their antipsychotic efficacy. The aliphatic linkers (1,3-propane-diyl and 1,4-butane-diyl) for new ligands were chosen based on previous studies [41,44]. These new derivatives were evaluated for their D<sub>2</sub>R antagonistic properties with the emphasis on the structure–activity relationships regarding the type of amine and length of the linker.

### 3.2. The Synthesis of Novel Compounds

The syntheses of novel analogues are depicted in Scheme 1. Nucleophilic addition of 1-bromo-3-chloropropane (**2**) or 1-bromo-4-chlorobutane (**3**) to the starting compound 3,4-dihydro-2(1*H*)-quinolinone (**1**, Scheme 1) in the presence of sodium hydride produced intermediates **4a,b** [42]. These derivatives were obtained in excellent yields (>70%). The final compounds **5a-g** and **6a-g** were prepared again by nucleophilic addition of the appropriate amine (**a-g**) to **4a,b** in the presence of K<sub>2</sub>CO<sub>3</sub> [46]. All the reactions exhibited good yields (>45%). The final products were analyzed by <sup>1</sup>H and <sup>13</sup>C NMR, HRMS and LC-MS analysis revealing the purity > 95%.



Scheme 1. Synthesis of new quinolinone derivatives **5a-g** and **6a-g**.

### 3.3. Binding Affinities of Novel Compounds at D<sub>2</sub>Rs and Their Cytotoxicities

The results of the affinity of **5a-g** and **6a-g** for D<sub>2</sub>R are summarized in Table 1. In general, 1,3-propane-diyl derivatives **5a-g** exhibited slightly better D<sub>2</sub>R antagonism than their 1,4-butane-diyl counterparts **6a-g**. The aliphatic analogues **5f,g** and **6g** possessed slightly lower D<sub>2</sub>R antagonism than the molecules with cyclic amines **5a-e** and **6a-c,e**. Morpholine-containing compound **6d** showed the lowest D<sub>2</sub>R antagonism from all cyclic amine derivatives (**5a-e** and **6a-e**). On the other hand, thiomorpholine analogue **5e** had the strongest antagonistic behavior at D<sub>2</sub>Rs from all prepared final compounds. Interestingly, the final derivatives **5a-g**, **6a-g** exhibited very low cytotoxicity in MTT (3-[4,5-dimethylthiazol-2-yl]-2,5-diphenyltetrazolium bromide) assay using Chinese hamster ovary cell lines (Table 1) so that the relatively lower affinity toward D<sub>2</sub>R is compensated by low toxicity allowing higher dosing.

**Table 1.** Binding affinity of tested final compounds **5a-g** and **6a-g** at D<sub>2</sub>Rs and their cytotoxicity.

Compound	K <sub>i</sub> (μM) ± SEM <sup>1</sup>	CHO-K1 IC <sub>50</sub> (mM) ± SEM <sup>2</sup>
<b>5a</b>	24 ± 5.8	2.0 ± 0.8
<b>5b</b>	9.7 ± 1.6	1.5 ± 0.3
<b>5c</b>	12 ± 3.2	2.0 ± 1.0
<b>5d</b>	20 ± 1.6	1.1 ± 0.3
<b>5e</b>	7.6 ± 1.9	0.5 ± 0.1
<b>5f</b>	37 ± 8.6	0.9 ± 0.2
<b>5g</b>	26 ± 6.1	1.5 ± 0.5
<b>6a</b>	23 ± 3.6	1.1 ± 0.2
<b>6b</b>	14 ± 2.5	0.8 ± 0.2
<b>6c</b>	21 ± 0.6	1.2 ± 0.2
<b>6d</b>	41 ± 14	1.3 ± 0.2
<b>6e</b>	9.7 ± 2.3	0.8 ± 0.1
<b>6f</b>	27 ± 4.7	1.8 ± 0.3
<b>6g</b>	45 ± 11	2.1 ± 0.8
Aripiprazole	3.3 nM <sup>3</sup>	0.1 <sup>4</sup>

<sup>1</sup> Values are expressed as mean ± SEM (μM) (*n* = 3). <sup>2</sup> The effect of the compounds on the cell viability. Values are expressed as the IC<sub>50</sub>: mean ± SEM (mM) (*n* = 3). <sup>3</sup> Please see paper by Shapiro et al. [54]. The value is K<sub>i</sub> value. <sup>4</sup> The effect of aripiprazole in MTT assay on NIH3T3 cell lines. The IC<sub>50</sub> value taken from ref. [81]. K<sub>D</sub> = 60 ± 2.8 pM (*n* = 6); B<sub>MAX</sub> = 2.0 ± 0.1 pmol/mg (*n* = 6).

### 3.4. Molecular Modelling Studies

A molecular modelling study was undertaken to help explain differences in binding strength. Quantitative results are summarized in Table 2, the docking score (S) and the calculated relative binding energy (ddG) from the thermodynamic integration free energy calculation follow the same tendency as the measured affinities. Docking of USC-D301 and **5e** revealed strongly differing binding poses, despite their high molecular similarity (Figure 2). The positively charged nitrogen of all docked ligands was recognized by Asp114 via a strong ionic ammonium-carboxylate interaction. A pi–pi interaction with Phe390 was also apparent, with the isoxazole, 2,3-dichlorophenyl and 2-methoxyphenyl fragment of risperidone, aripiprazole, and USC-D301, respectively. Surprisingly, the lowest scoring docking pose of **5e** did not overlap with USC-D301 (Figure 3). Owing to its smaller size and thiomorpholine cap, there is no aromatic group at that position that can undergo the stacking interaction with Phe390 or other nearby residues, likely leading to a strong penalty to the binding energy. Instead, the molecule adopts a flipped conformation that places the benzolactam fragment in this pocket, where the fused benzene ring is not positioned well to undergo stacking with Phe390, Trp386, and others.

**Table 2.** Results for molecular studies.

Ligand	S (Docking Score, kcal/mol)	ddG (Relative Free Energy, kcal/mol)
risperidone	−9.6461	−10.0988
aripiprazole	−9.1619	−10.2544
USC-D301	−8.4562	−9.5903
<b>5e</b>	−7.0336	−8.2686

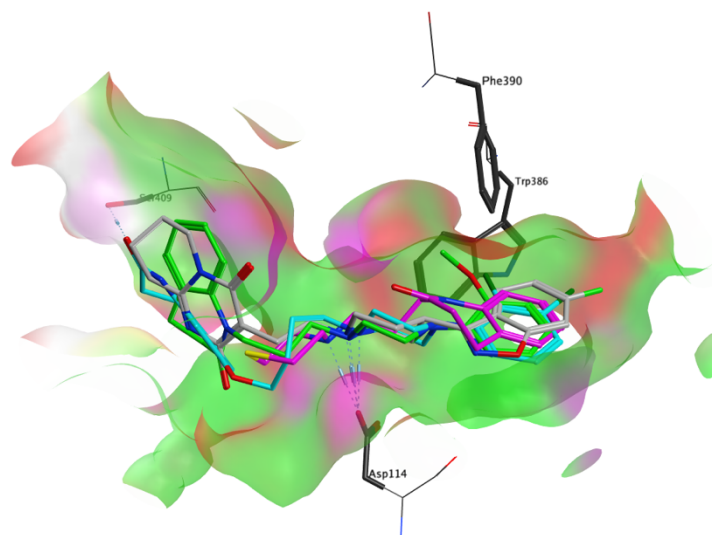


**Figure 2.** All four ligands with docked poses in the binding pocket with different rendering style (grey: risperidone, cyan: aripiprazole, green: USC-D301, purple: **5e**). Surface color of pocket: green is hydrophobic, purple is polar, and red is exposed. For clarity, only residues that showed selective interactions in the docking screens are rendered, sidechains in bold.

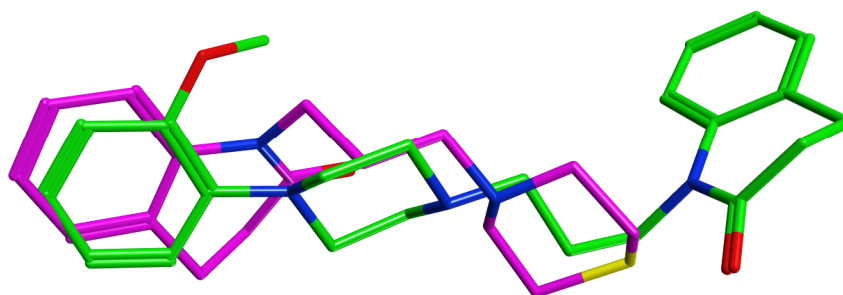


**Figure 3.** Closer view of the 3D overlay of the final docked conformations of USC-D301 (green) and **5e** (purple). Despite their chemical similarity, there is no alignment.

### 3.5. Central Nervous System Availability Prediction and Study for Novel Compounds

Before the synthesis, we have calculated the so-called BBB score to predict the compound's CNS availability. Indeed, all the compounds displayed high values above 5.0 (5.2–5.4) which is indicative of their high potential to cross BBB. The prediction was then confirmed by the data from parallel artificial membrane permeation (PAMPA) assay pointing out their potential to cross the BBB by passive diffusion (**5a-g** and **6a-g**  $P_e$  ( $\times 10^{-6} \text{ cm s}^{-1}$ ) = 7.0–24) (Table 3). The validation of PAMPA has been performed using standard compounds whose availability or unavailability was experimentally predicted in vitro and confirmed in vivo [53,82].

**Table 3.** Prediction of BBB barrier penetration of the studied compounds expressed as  $P_e$  ( $n = 3$ ) and BBB score of final derivatives.

Compound	BBB Score <sup>1</sup>	$P_e \pm \text{SEM} (\times 10^{-6} \text{ cm s}^{-1})$	CNS (+/−) <sup>2</sup>
5a	5.3	7.3 ± 0.8	CNS +
5b	5.2	13 ± 0.1	CNS +
5c	5.4	7.0 ± 0.4	CNS +
5d	5.2	12 ± 2.0	CNS +
5e	5.2	24 ± 2.1	CNS +
5f	5.2	9.4 ± 0.4	CNS +
5g	5.3	10 ± 1.6	CNS +
6a	5.2	7.7 ± 1.8	CNS +
6b	5.2	10 ± 1.4	CNS +
6c	5.4	7.1 ± 1.2	CNS +
6d	5.3	17 ± 2.1	CNS +
6e	5.2	23 ± 3.3	CNS +
6f	5.2	7.4 ± 0.9	CNS +
6g	5.3	9.5 ± 1.1	CNS +
Donepezil	5.3	22 ± 2.1	CNS +
Tacrine	5.4	6.0 ± 0.6	CNS +
Rivastigmine	5.1	20 ± 2.1	CNS +
Furosemide	-	0.2 ± 0.1	CNS −
Chlorothiazide	-	1.2 ± 0.5	CNS −
Ranitidine	-	0.4 ± 0.3	CNS −

<sup>1</sup> Ligands exhibiting BBB score of 4–5 have 54.5% probability to cross BBB; score ranging between 5–6 indicates 90.3% probability of potential central activity [49]; <sup>2</sup> CNS + (high BBB permeability predicted),  $P_e (10^{-6} \text{ cm}\cdot\text{s}^{-1}) > 4.0$ ; CNS − (low BBB permeability predicted),  $P_e (10^{-6} \text{ cm}\cdot\text{s}^{-1}) < 2.0$ ; CNS +/- (BBB permeability uncertain),  $P_e (10^{-6} \text{ cm}\cdot\text{s}^{-1})$  from 4.0 to 2.0 [53].

#### 4. Conclusions

In summary, a series of 3,4-dihydroquinolin-2(1*H*)-one analogues, inspired by aripiprazole was designed and synthesized. The substitutions of the amine group revealed a negligible impact on D<sub>2</sub>R affinity. Although the binding affinities at D<sub>2</sub>Rs of new analogues are much weaker compared to aripiprazole, they are very close to the binding affinity, for instance, of memantine acting as *N*-methyl-D-aspartate receptor antagonist, a well-established drug for the treatment of Alzheimer’s disease [83,84]. Out of these ligands, **5e** possessed the highest D<sub>2</sub>R affinity, very low cytotoxicity profile, and the highest probability to cross the BBB. Molecular modeling simulation revealed completely different binding mode of **5e** compared to USC-D301, which might be the culprit of the reduced affinity of **5e** toward D<sub>2</sub>R. The subject of further investigation of these compounds will be to assess their affinity toward other members of the D<sub>2</sub>-like receptors family and other GPCRs, especially 5-HT<sub>1A</sub> and 5-HT<sub>2A</sub>Rs. Since aripiprazole has few of the typical adverse effects of other antipsychotics, such as extrapyramidal symptoms, hyperprolactinemia, weight gain, metabolic disorders, and sedation given to its unique biased activity and/or partial agonistic/antagonistic actions on D<sub>2</sub>Rs supplemented by the action on other dopamine receptor subtypes (mainly D<sub>3</sub>R) and 5-HT receptor subtypes (mainly 5-HT<sub>1A</sub>, 5-HT<sub>2A</sub>) [54], the ongoing study must determine the functional affinity of newly developed compounds at these receptors to evaluate the real antipsychotic effect and clinical potential [85].



**Supplementary Materials:** The following are available online at <https://www.mdpi.com/article/10.3390/biom11091262/s1>. Figure S1:  $^1\text{H}$  NMR spectrum for **5a**. Figure S2:  $^{13}\text{C}$  NMR spectrum for **5a**. Figure S3: UV-LC chromatogram for **5a**. Figure S4: HRMS spectrum for **5a**. Figure S5:  $^1\text{H}$  NMR spectrum for **5b**. Figure S6:  $^{13}\text{C}$  NMR spectrum for **5b**. Figure S7: UV-LC chromatogram for **5b**. Figure S8: HRMS spectrum for **5b**. Figure S9:  $^1\text{H}$  NMR spectrum for **5c**. Figure S10:  $^{13}\text{C}$  NMR spectrum for **5c**. Figure S11: UV-LC chromatogram for **5c**. Figure S12: HRMS spectrum for **5c**. Figure S13:  $^1\text{H}$  NMR spectrum for **5d**. Figure S14:  $^{13}\text{C}$  NMR spectrum for **5d**. Figure S15: UV-LC chromatogram for **5d**. Figure S16: HRMS spectrum for **5d**. Figure S17:  $^1\text{H}$  NMR spectrum for **5e**. Figure S18:  $^{13}\text{C}$  NMR spectrum for **5e**. Figure S19: UV-LC chromatogram for **5e**. Figure S20: HRMS spectrum for **5e**. Figure S21:  $^1\text{H}$  NMR spectrum for **5f**. Figure S22:  $^{13}\text{C}$  NMR spectrum for **5f**. Figure S23: UV-LC chromatogram for **5f**. Figure S24: HRMS spectrum for **5f**. Figure S25:  $^1\text{H}$  NMR spectrum for **5g**. Figure S26:  $^{13}\text{C}$  NMR spectrum for **5g**. Figure S27: UV-LC chromatogram for **5g**. Figure S28: HRMS spectrum for **5g**. Figure S29:  $^1\text{H}$  NMR spectrum for **6a**. Figure S30:  $^{13}\text{C}$  NMR spectrum for **6a**. Figure S31: UV-LC chromatogram for **6a**. Figure S32: HRMS spectrum for **6a**. Figure S33:  $^1\text{H}$  NMR spectrum for **6b**. Figure S34:  $^{13}\text{C}$  NMR spectrum for **6b**. Figure S35: UV-LC chromatogram for **6b**. Figure S36: HRMS spectrum for **6b**. Figure S37:  $^1\text{H}$  NMR spectrum for **6c**. Figure S38:  $^{13}\text{C}$  NMR spectrum for **6c**. Figure S39: UV-LC chromatogram for **6c**. Figure S40: HRMS spectrum for **6c**. Figure S41:  $^1\text{H}$  NMR spectrum for **6d**. Figure S42:  $^{13}\text{C}$  NMR spectrum for **6d**. Figure S43: UV-LC chromatogram for **6d**. Figure S44: HRMS spectrum for **6d**. Figure S45:  $^1\text{H}$  NMR spectrum for **6e**. Figure S46:  $^{13}\text{C}$  NMR spectrum for **6e**. Figure S47: UV-LC chromatogram for **6e**. Figure S48: HRMS spectrum for **6e**. Figure S49:  $^1\text{H}$  NMR spectrum for **6f**. Figure S50:  $^{13}\text{C}$  NMR spectrum for **6f**. Figure S51: UV-LC chromatogram for **6f**. Figure S52: HRMS spectrum for **6f**. Figure S53:  $^1\text{H}$  NMR spectrum for **6g**. Figure S54:  $^{13}\text{C}$  NMR spectrum for **6g**. Figure S55: UV-LC chromatogram for **6g**. Figure S56: HRMS spectrum for **6g**. Figure S57: Saturation binding curve and Scatchard plot of the affinity of [ $^3\text{H}$ ]spiperone to  $\text{D}_2\text{Rs}$ . Figure S58: Inhibition of [ $^3\text{H}$ ]spiperone binding to  $\text{D}_2\text{RS}$  receptors by 3,4-dihydroquinolin-2(1H)-one derivatives (**5a-g**). Figure S59: Inhibition of [ $^3\text{H}$ ]spiperone binding to  $\text{D}_2\text{RS}$  receptors by 3,4-dihydroquinolin-2(1H)-one derivatives (**6a-g**). Figure S60: Schematic representation of the settings used in the Thermodynamic Integration Free Energy Calculation. Table S1: Functional activities of **5a-g** and **6a-g** at  $\text{D}_2\text{Rs}$ .

**Author Contributions:** R.J. and E.M. chemical synthesis and writing the paper; K.S. and A.R. binding affinity studies; W.D. molecular modelling studies; L.P. (Lukas Prchal) HRMS and LC-MS analysis; L.P. (Lenka Pulkrabkova), T.K., L.M. cell experiments; M.M. blood–brain barrier prediction; K.M., O.S. and J.K. designed the study; T.P., I.V., O.S. and JK reviewed and edited the paper; K.M., J.K. and O.S. funding acquisition. All authors have read and agreed to the published version of the manuscript.

**Funding:** W.D. was supported by the Ministry of Education, Youth and Sports of the Czech Republic, project number LM2018130. The work was supported by the Czech Science Foundation (No. 19-11332S) and University of Hradec Kralove (No. SV2104-2021 and VT2019-2021).

**Institutional Review Board Statement:** Not applicable.

**Informed Consent Statement:** Not applicable.

**Data Availability Statement:** The compounds developed within this study are available from the corresponding author on reasonable request.

**Conflicts of Interest:** The authors declare no conflict of interest.

## References

1. Matt, S.M.; Gaskill, P.J. Where Is Dopamine and How Do Immune Cells See It? Dopamine-Mediated Immune Cell Function in Health and Disease. *J. Neuroimmune Pharm.* **2020**, *15*, 114–164. [[CrossRef](#)] [[PubMed](#)]
2. Ayano, G. Dopamine: Receptors, Functions, Synthesis, Pathways, Locations and Mental Disorders: Review of Literatures. *J. Ment. Disord. Treat.* **2016**, *2*. [[CrossRef](#)]
3. Klein, M.O.; Battagello, D.S.; Cardoso, A.R.; Hauser, D.N.; Bittencourt, J.C.; Correa, R.G. Dopamine: Functions, Signaling, and Association with Neurological Diseases. *Cell. Mol. Neurobiol.* **2019**, *39*, 31–59. [[CrossRef](#)] [[PubMed](#)]
4. Martel, J.C.; Gatti McArthur, S. Dopamine Receptor Subtypes, Physiology and Pharmacology: New Ligands and Concepts in Schizophrenia. *Front. Pharmacol.* **2020**, *11*, 1003. [[CrossRef](#)] [[PubMed](#)]
5. Pivonello, R.; Ferone, D.; Lombardi, G.; Colao, A.; Lamberts, S.W.J.; Hofland, L.J. Novel Insights in Dopamine Receptor Physiology. *Eur. J. Endocrinol.* **2007**, *156*, S13–S21. [[CrossRef](#)]

6. Żuk, J.; Bartuzi, D.; Matosiuk, D.; Kaczor, A.A. Preferential Coupling of Dopamine D2S and D2L Receptor Isoforms with Gi1 and Gi2 Proteins—In Silico Study. *Int. J. Mol. Sci.* **2020**, *21*, 436. [[CrossRef](#)] [[PubMed](#)]
7. Usiello, A.; Baik, J.H.; Rougé-Pont, F.; Picetti, R.; Dierich, A.; LeMeur, M.; Piazza, P.V.; Borrelli, E. Distinct Functions of the Two Isoforms of Dopamine D2 Receptors. *Nature* **2000**, *408*, 199–203. [[CrossRef](#)] [[PubMed](#)]
8. Beaulieu, J.-M.; Gainetdinov, R.R. The Physiology, Signaling, and Pharmacology of Dopamine Receptors. *Pharm. Rev.* **2011**, *63*, 182–217. [[CrossRef](#)]
9. Stepnicki, P.; Kondej, M.; Kaczor, A.A. Current Concepts and Treatments of Schizophrenia. *Molecules* **2018**, *23*, 2087. [[CrossRef](#)]
10. Wang, S.-M.; Han, C.; Lee, S.-J.; Jun, T.-Y.; Patkar, A.A.; Masand, P.S.; Pae, C.-U. Second Generation Antipsychotics in the Treatment of Major Depressive Disorder: An Update. *Chonnam. Med. J.* **2016**, *52*, 159–172. [[CrossRef](#)]
11. Mulder, R.; Hamilton, A.; Irwin, L.; Boyce, P.; Morris, G.; Porter, R.J.; Malhi, G.S. Treating Depression with Adjunctive Antipsychotics. *Bipolar Disord.* **2018**, *20*, 17–24. [[CrossRef](#)] [[PubMed](#)]
12. Hershenberg, R.; Gros, D.F.; Brawman-Mintzer, O. Role of Atypical Antipsychotics in the Treatment of Generalized Anxiety Disorder. *CNS Drugs* **2014**, *28*, 519–533. [[CrossRef](#)]
13. Pignon, B.; Montcel, C.T.; Carton, L.; Pelissolo, A. The Place of Antipsychotics in the Therapy of Anxiety Disorders and Obsessive-Compulsive Disorders. *Curr. Psychiatry Rep.* **2017**, *19*, 1–11. [[CrossRef](#)] [[PubMed](#)]
14. Marder, S.R.; Cannon, T.D. Schizophrenia. *N. Engl. J. Med.* **2019**, *381*, 1753–1761. [[CrossRef](#)] [[PubMed](#)]
15. Radhakrishnan, R.; Kaser, M.; Guloksuz, S. The Link Between the Immune System, Environment, and Psychosis. *Schizophr. Bull.* **2017**, *43*, 693–697. [[CrossRef](#)] [[PubMed](#)]
16. Laruelle, M. Schizophrenia: From Dopaminergic to Glutamatergic Interventions. *Curr. Opin. Pharmacol.* **2014**, *14*, 97–102. [[CrossRef](#)]
17. McCutcheon, R.A.; Abi-Dargham, A.; Howes, O.D. Schizophrenia, Dopamine and the Striatum: From Biology to Symptoms. *Trends Neurosci.* **2019**, *42*, 205–220. [[CrossRef](#)]
18. Kapur, S.; Zipursky, R.; Jones, C.; Remington, G.; Houle, S. Relationship Between Dopamine D2 Occupancy, Clinical Response, and Side Effects: A Double-Blind PET Study of First-Episode Schizophrenia. *AJP* **2000**, *157*, 514–520. [[CrossRef](#)]
19. Nordström, A.-L.; Farde, L.; Wiesel, F.-A.; Forslund, K.; Pauli, S.; Halldin, C.; Uppfeldt, G. Central D2-Dopamine Receptor Occupancy in Relation to Antipsychotic Drug Effects: A Double-Blind PET Study of Schizophrenic Patients. *Biol. Psychiatry* **1993**, *33*, 227–235. [[CrossRef](#)]
20. Richtand, N.M.; Welge, J.A.; Logue, A.D.; Keck, P.E.; Strakowski, S.M.; McNamara, R.K. Dopamine and Serotonin Receptor Binding and Antipsychotic Efficacy. *Neuropsychopharmacology* **2007**, *32*, 1715–1726. [[CrossRef](#)]
21. Seeman, P.; Lee, T.; Chau-Wong, M.; Wong, K. Antipsychotic Drug Doses and Neuroleptic/Dopamine Receptors. *Nature* **1976**, *261*, 717–719. [[CrossRef](#)]
22. Karlsson, P.; Farde, L.; Härnryd, C.; Sedvall, G.; Smith, L.; Wiesel, F.-A. Lack of Apparent Antipsychotic Effect of the D<sub>1</sub>-Dopamine Receptor Antagonist SCH39166 in Acutely Ill Schizophrenic Patients. *Psychopharmacology* **1995**, *121*, 309–316. [[CrossRef](#)] [[PubMed](#)]
23. Redden, L.; Rendenbach-Mueller, B.; Abi-Saab, W.; Katz, D.; Goenjian, A.; Robieson, W.; Wang, Y.; Goss, S.; Greco, N.; Saltarelli, M. A Double-Blind, Randomized, Placebo-Controlled Study of the Dopamine D-3 Receptor Antagonist ABT-925 in Patients With Acute Schizophrenia. *J. Clin. Psychopharmacol.* **2011**, *31*, 221–225. [[CrossRef](#)] [[PubMed](#)]
24. Bristow, L.J.; Kramer, M.S.; Kulagowski, J.; Patel, S.; Ragan, C.I.; Seabrook, G.R. Schizophrenia and L-745, 870, a Novel Dopamine D4 Receptor Antagonist. *Trends Pharmacol. Sci.* **1997**, *18*, 186–188. [[CrossRef](#)]
25. George, M.S.; Molnar, C.E.; Grenesko, E.L.; Anderson, B.; Mu, Q.; Johnson, K.; Nahas, Z.; Knable, M.; Fernandes, P.; Juncos, J.; et al. A Single 20 Mg Dose of Dihydroxidine (DAR-0100), a Full Dopamine D1 Agonist, Is Safe and Tolerated in Patients with Schizophrenia. *Schizophr. Res.* **2007**, *93*, 42–50. [[CrossRef](#)]
26. Girgis, R.R.; Van Snellenberg, J.X.; Glass, A.; Kegeles, L.S.; Thompson, J.L.; Wall, M.; Cho, R.Y.; Carter, C.S.; Slifstein, M.; Abi-Dargham, A.; et al. A Proof-of-Concept, Randomized Controlled Trial of DAR-0100A, a Dopamine-1 Receptor Agonist, for Cognitive Enhancement in Schizophrenia. *J. Psychopharmacol.* **2016**, *30*, 428–435. [[CrossRef](#)]
27. Rosell, D.; Zaluda, L.; McClure, M.; Perez-Rodriguez, M.; Strike, S.; Barch, D.; Harvey, P.; Girgis, R.; Hazlett, E.; Mailman, R.; et al. Effects of the D1 Dopamine Receptor Agonist Dihydroxidine (DAR-0100A) on Working Memory in Schizotypal Personality Disorder. *Neuropsychopharmacology* **2015**, *40*, 446–453. [[CrossRef](#)]
28. Zheng, W.; Li, X.H.; Cai, D.B.; Yang, X.H.; Ungvari, G.S.; Ng, C.H.; Ning, Y.P.; Xiang, Y.T. Adjunctive Azapirone for Schizophrenia: A Meta-Analysis of Randomized, Double-Blind, Placebo-Controlled Trials. *Eur. Neuropsychopharmacol.* **2018**, *28*, 149–158. [[CrossRef](#)]
29. Meltzer, H.; Huang, M. In Vivo Actions of Atypical Antipsychotic Drug on Serotonergic and Dopaminergic Systems. *Prog. Brain Res.* **2008**, *172*, 177–197. [[CrossRef](#)] [[PubMed](#)]
30. Kaar, S.J.; Natesan, S.; McCutcheon, R.; Howes, O.D. Antipsychotics: Mechanisms Underlying Clinical Response and Side-Effects and Novel Treatment Approaches Based on Pathophysiology. *Neuropharmacology* **2020**, *172*, 107704. [[CrossRef](#)]
31. Richelson, E.; Souder, T. Binding of Antipsychotic Drugs to Human Brain Receptors Focus on Newer Generation Compounds. *Life Sci.* **2000**, *68*, 29–39. [[CrossRef](#)]
32. Schneider, L.S. Pimavanserin for Patients with Alzheimer’s Disease Psychosis. *Lancet Neurol.* **2018**, *17*, 194–195. [[CrossRef](#)]

33. Bebawy, M.; Chetty, M. Differential Pharmacological Regulation of Drug Efflux and Pharmacoresistant Schizophrenia. *BioEssays* **2008**, *30*, 183–188. [CrossRef] [PubMed]
34. Carbon, M.; Correll, C.U. Thinking and Acting beyond the Positive: The Role of the Cognitive and Negative Symptoms in Schizophrenia. *CNS Spectr.* **2014**, *19*, 35–53. [CrossRef]
35. De Berardis, D.; Rapini, G.; Olivieri, L.; Di Nicola, D.; Tomasetti, C.; Valchera, A.; Fornaro, M.; Di Fabio, F.; Perna, G.; Di Nicola, M.; et al. Safety of Antipsychotics for the Treatment of Schizophrenia: A Focus on the Adverse Effects of Clozapine. *Adv. Drug Saf.* **2018**, *9*, 237–256. [CrossRef] [PubMed]
36. Weston-Green, K.; Huang, X.-F.; Deng, C. Second Generation Antipsychotic-Induced Type 2 Diabetes: A Role for the Muscarinic M3 Receptor. *CNS Drugs* **2013**, *27*, 1069–1080. [CrossRef]
37. Osuch, E.; Marais, A. The Pharmacological Management of Depression—Update 2017. *South Afr. Fam. Pract.* **2017**, *59*, 6–16. [CrossRef]
38. Bystritsky, A.; Khalsa, S.S.; Cameron, M.E.; Schiffman, J. Current Diagnosis and Treatment of Anxiety Disorders. *Pharm. Ther.* **2013**, *38*, 30–57.
39. Gustavsson, A.; Svensson, M.; Jacobi, F.; Allgulander, C.; Alonso, J.; Beghi, E.; Dodel, R.; Ekman, M.; Faravelli, C.; Fratiglioni, L.; et al. Cost of Disorders of the Brain in Europe 2010. *Eur. Neuropsychopharmacol.* **2011**, *21*, 718–779. [CrossRef]
40. Wood, M.; Reavill, C. Aripiprazole Acts as a Selective Dopamine D2 Receptor Partial Agonist. *Expert Opin. Investig. Drugs* **2007**, *16*, 771–775. [CrossRef]
41. López, L.; Selent, J.; Ortega, R.; Masaguer, C.F.; Domínguez, E.; Areias, F.; Brea, J.; Loza, M.I.; Sanz, F.; Pastor, M. Synthesis, 3D-QSAR, and Structural Modeling of Benzolactam Derivatives with Binding Affinity for the D2 and D3 Receptors. *ChemMedChem* **2010**, *5*, 1300–1317. [CrossRef]
42. Niso, M.; Pati, M.L.; Berardi, F.; Abate, C. Rigid versus Flexible Anilines or Anilides Confirm the Bicyclic Ring as the Hydrophobic Portion for Optimal  $\Sigma 2$  Receptor Binding and Provide Novel Tools for the Development of Future  $\Sigma 2$  Receptor PET Radiotracers. *RSC Adv.* **2016**, *6*, 88508–88518. [CrossRef]
43. Skjaerback, N.; Koch, K.N.; Friberg, B.L.M.; Tolf, B.-R. Tetrahydroquinoline Analogues as Muscarinic Agonists. WO2003057672A3, 13 November 2003.
44. Geneste, H.; Backfisch, G.; Braje, W.; Delzer, J.; Haupt, A.; Hutchins, C.W.; King, L.L.; Lubisch, W.; Steiner, G.; Teschendorf, H.-J.; et al. Synthesis and SAR of Highly Potent and Selective Dopamine D3-Receptor Antagonists: Quinolin(Di)One and Benzazepin(Di)One Derivatives. *Bioorganic Med. Chem. Lett.* **2006**, *16*, 658–662. [CrossRef]
45. Oshiro, Y.; Sakurai, Y.; Sato, S.; Kurahashi, N.; Tanaka, T.; Kikuchi, T.; Tottori, K.; Uwahodo, Y.; Miwa, T.; Nishi, T. 3,4-Dihydro-2(1H)-Quinolinone as a Novel Antidepressant Drug: Synthesis and Pharmacology of 1-[3-[4-(3-Chlorophenyl)-1-Piperazinyl]Propyl]-3,4-Dihydro-5-Methoxy-2(1H)-Quinolinone and Its Derivatives. *J. Med. Chem.* **2000**, *43*, 177–189. [CrossRef] [PubMed]
46. Shi, W.; Wang, Y.; Wu, C.; Yang, F.; Zheng, W.; Wu, S.; Liu, Y.; Wang, Z.; He, Y.; Shen, J. Synthesis and Biological Investigation of Triazolopyridinone Derivatives as Potential Multireceptor Atypical Antipsychotics. *Bioorganic Med. Chem. Lett.* **2020**, *30*, 127027. [CrossRef] [PubMed]
47. Chemical Computing Group ULC. *Molecular Operating Environment (MOE)*. 2019. Available online: [https://www.chemcomp.com/Research-Citing\\_MOE.htm](https://www.chemcomp.com/Research-Citing_MOE.htm) (accessed on 16 June 2021).
48. Wang, S.; Che, T.; Levit, A.; Shoichet, B.K.; Wacker, D.; Roth, B.L. Structure of the D2 Dopamine Receptor Bound to the Atypical Antipsychotic Drug Risperidone. *Nature* **2018**, *555*, 269–273. [CrossRef]
49. Gupta, M.; Lee, H.J.; Barden, C.J.; Weaver, D.F. The Blood–Brain Barrier (BBB) Score. *J. Med. Chem.* **2019**, *62*, 9824–9836. [CrossRef] [PubMed]
50. El-Fakahany, E.E.; Jakubik, J. Radioligand Binding at Muscarinic Receptors. In *Muscarinic Receptor: From Structure to Animal Models*; Myslivecek, J., Jakubik, J., Eds.; Neuromethods; Springer: New York, NY, USA, 2016; pp. 37–68. ISBN 978-1-4939-2858-3.
51. Peterson, G.L. A Simplification of the Protein Assay Method of Lowry et Al. Which Is More Generally Applicable. *Anal. Biochem.* **1977**, *83*, 346–356. [CrossRef]
52. Malinak, D.; Dolezal, R.; Marek, J.; Salajkova, S.; Soukup, O.; Vejsova, M.; Korabecny, J.; Honegr, J.; Penhaker, M.; Musilek, K.; et al. 6-Hydroxyquinolinium Salts Differing in the Length of Alkyl Side-Chain: Synthesis and Antimicrobial Activity. *Bioorganic Med. Chem. Lett.* **2014**, *24*, 5238–5241. [CrossRef] [PubMed]
53. Di, L.; Kerns, E.H.; Fan, K.; McConnell, O.J.; Carter, G.T. High Throughput Artificial Membrane Permeability Assay for Blood–brain Barrier. *Eur. J. Med. Chem.* **2003**, *38*, 223–232. [CrossRef]
54. Shapiro, D.A.; Renock, S.; Arrington, E.; Chiodo, L.A.; Liu, L.-X.; Sibley, D.R.; Roth, B.L.; Mailman, R.; Aripiprazole, A. Novel Atypical Antipsychotic Drug with a Unique and Robust Pharmacology. *Neuropsychopharmacology* **2003**, *28*, 1400–1411. [CrossRef]
55. Pae, C.-U.; Forbes, A.; Patkar, A. Aripiprazole as Adjunctive Therapy for Patients with Major Depressive Disorder. *CNS Drugs* **2011**, *25*, 109–127. [CrossRef] [PubMed]
56. Jauhar, S.; Young, A.H. Controversies in Bipolar Disorder; Role of Second-Generation Antipsychotic for Maintenance Therapy. *Int. J. Bipolar Disord.* **2019**, *7*, 1–9. [CrossRef]
57. Brust, T.F.; Hayes, M.P.; Roman, D.L.; Watts, V.J. New Functional Activity of Aripiprazole Revealed: Robust Antagonism of D2 Dopamine Receptor-Stimulated G $\beta\gamma$  Signaling. *Biochem. Pharmacol.* **2015**, *93*, 85–91. [CrossRef] [PubMed]



58. Allen, J.A.; Yost, J.M.; Setola, V.; Chen, X.; Sassano, M.F.; Chen, M.; Peterson, S.; Yadav, P.N.; Huang, X.; Feng, B.; et al. Discovery of  $\beta$ -Arrestin-Biased Dopamine D2 Ligands for Probing Signal Transduction Pathways Essential for Antipsychotic Efficacy. *Proc. Natl. Acad. Sci. USA* **2011**, *108*, 18488–18493. [[CrossRef](#)] [[PubMed](#)]
59. Mailman, R.B.; Murthy, V. Third Generation Antipsychotic Drugs: Partial Agonism or Receptor Functional Selectivity? *Curr. Pharm. Des.* **2010**, *16*, 488–501. [[CrossRef](#)] [[PubMed](#)]
60. Lieberman, J.A. Dopamine Partial Agonists. *CNS Drugs* **2004**, *18*, 251–267. [[CrossRef](#)] [[PubMed](#)]
61. Keck, P.E., Jr.; McElroy, S.L. Aripiprazole: A Partial Dopamine D2 Receptor Agonist Antipsychotic. *Expert Opin. Investig. Drugs* **2003**, *12*, 655–662. [[CrossRef](#)]
62. Löber, S.; Hübner, H.; Tschammer, N.; Gmeiner, P. Recent Advances in the Search for D3- and D4-Selective Drugs: Probes, Models and Candidates. *Trends Pharmacol. Sci.* **2011**, *32*, 148–157. [[CrossRef](#)]
63. Bettinetti, L.; Schlotter, K.; Hübner, H.; Gmeiner, P. Interactive SAR Studies: Rational Discovery of Super-Potent and Highly Selective Dopamine D3 Receptor Antagonists and Partial Agonists. *J. Med. Chem.* **2002**, *45*, 4594–4597. [[CrossRef](#)]
64. Ehrlich, K.; Götz, A.; Bollinger, S.; Tschammer, N.; Härterich, S.; Hübner, H.; Lanig, H.; Gmeiner, P. Dopamine D2, D3, and D4 Selective Phenylpiperazines as Molecular Probes To Explore the Origins of Subtype Specific Receptor Binding. *J. Med. Chem.* **2009**, *52*, 4923–4935. [[CrossRef](#)] [[PubMed](#)]
65. De Simone, A.; Russo, D.; Ruda, G.F.; Micoli, A.; Ferraro, M.; Di Martino, R.M.C.; Ottonello, G.; Summa, M.; Armirotti, A.; Bandiera, T.; et al. Design, Synthesis, Structure–Activity Relationship Studies, and Three-Dimensional Quantitative Structure–Activity Relationship (3D-QSAR) Modeling of a Series of O-Biphenyl Carbamates as Dual Modulators of Dopamine D3 Receptor and Fatty Acid Amide Hydrolase. *J. Med. Chem.* **2017**, *60*, 2287–2304. [[CrossRef](#)]
66. Żmudzki, P.; Satała, G.; Bojarski, A.; Chłóń-Rzepa, G.; Popik, P.; Zajdel, P. N-(4-Arylpiperazinoalkyl)Acetamide Derivatives of 1,3- and 3,7-Dimethyl-1H-Purine-2,6(3H,7H)-Diones and Their 5-HT<sub>6</sub>, 5-HT<sub>7</sub>, and D2 Receptors Affinity. *Heterocycl. Commun.* **2015**, *21*, 13–18. [[CrossRef](#)]
67. Banala, A.K.; Levy, B.A.; Khatri, S.S.; Furman, C.A.; Roof, R.A.; Mishra, Y.; Griffin, S.A.; Sibley, D.R.; Luedtke, R.R.; Newman, A.H. N-(3-Fluoro-4-(4-(2-Methoxy or 2,3-Dichlorophenyl) Piperazine-1-Yl)-Butyl)-Aryl Carboxamides as Selective Dopamine D3 Receptor Ligands: Critical Role of the Carboxamide Linker for D3 Receptor Selectivity. *J. Med. Chem.* **2011**, *54*, 3581–3594. [[CrossRef](#)]
68. Chen, X.; Sassano, M.F.; Zheng, L.; Setola, V.; Chen, M.; Bai, X.; Frye, S.V.; Wetsel, W.C.; Roth, B.L.; Jin, J. Structure-Functional Selectivity Relationship Studies of  $\beta$ -Arrestin-Biased Dopamine D2 Receptor Agonists. *J. Med. Chem.* **2012**, *55*, 7141–7153. [[CrossRef](#)]
69. Chen, X.; McCorvy, J.D.; Fischer, M.G.; Butler, K.V.; Shen, Y.; Roth, B.L.; Jin, J. Discovery of G Protein-Biased D2 Dopamine Receptor Partial Agonists. *J. Med. Chem.* **2016**, *59*, 10601–10618. [[CrossRef](#)]
70. Simone, A.D.; Ruda, G.F.; Albani, C.; Tarozzo, G.; Bandiera, T.; Piomelli, D.; Cavalli, A.; Bottegoni, G. Applying a Multitarget Rational Drug Design Strategy: The First Set of Modulators with Potent and Balanced Activity toward Dopamine D3 Receptor and Fatty Acid Amide Hydrolase. *Chem. Commun.* **2014**, *50*, 4904–4907. [[CrossRef](#)]
71. Vangveravong, S.; Zhang, Z.; Taylor, M.; Bearden, M.; Xu, J.; Cui, J.; Wang, W.; Luedtke, R.R.; Mach, R.H. Synthesis and Characterization of Selective Dopamine D2 Receptor Ligands Using Aripiprazole as the Lead Compound. *Bioorg. Med. Chem.* **2011**, *19*, 3502–3511. [[CrossRef](#)]
72. Männel, B.; Dengler, D.; Shonberg, J.; Hübner, H.; Möller, D.; Gmeiner, P. Hydroxy-Substituted Heteroaryl piperazines: Novel Scaffolds for  $\beta$ -Arrestin-Biased D2R Agonists. *J. Med. Chem.* **2017**, *60*, 4693–4713. [[CrossRef](#)]
73. Del Bello, F.; Bonifazi, A.; Giorgioni, G.; Cifani, C.; Micioni Di Bonaventura, M.V.; Petrelli, R.; Piergentili, A.; Fontana, S.; Mammoli, V.; Yano, H.; et al. 1-[3-(4-Butylpiperidin-1-Yl)Propyl]-1,2,3,4-Tetrahydroquinolin-2-One (77-LH-28-1) as a Model for the Rational Design of a Novel Class of Brain Penetrant Ligands with High Affinity and Selectivity for Dopamine D4 Receptor. *J. Med. Chem.* **2018**, *61*, 3712–3725. [[CrossRef](#)]
74. Martelle, J.L.; Nader, M.A. A Review of the Discovery, Pharmacological Characterization, and Behavioral Effects of the Dopamine D2-Like Receptor Antagonist Eticlopride. *CNS Neurosci.* **2008**, *14*, 248–262. [[CrossRef](#)] [[PubMed](#)]
75. Farde, L.; Wiesel, F.-A.; Halldin, C.; Sedvall, G. Central D2-Dopamine Receptor Occupancy in Schizophrenic Patients Treated With Antipsychotic Drugs. *Arch. Gen. Psychiatry* **1988**, *45*, 71–76. [[CrossRef](#)]
76. Farde, L.; Nordström, A.-L.; Wiesel, F.-A.; Pauli, S.; Halldin, C.; Sedvall, G. Positron Emission Tomographic Analysis of Central D1 and D2 Dopamine Receptor Occupancy in Patients Treated With Classical Neuroleptics and Clozapine: Relation to Extrapyramidal Side Effects. *Arch. Gen. Psychiatry* **1992**, *49*, 538–544. [[CrossRef](#)]
77. Kapur, S.; Zipursky, R.; Roy, P.; Jones, C.; Remington, G.; Reed, K.; Houle, S. The Relationship between D2 Receptor Occupancy and Plasma Levels on Low Dose Oral Haloperidol: A PET Study. *Psychopharmacology* **1997**, *131*, 148–152. [[CrossRef](#)]
78. Kapur, S.; Zipursky, R.B.; Remington, G. Clinical and Theoretical Implications of 5-HT<sub>2</sub> and D2 Receptor Occupancy of Clozapine, Risperidone, and Olanzapine in Schizophrenia. *AJP* **1999**, *156*, 286–293. [[CrossRef](#)]
79. Pilowsky, L.S.; Costa, D.C.; Ell, P.J.; Murray, R.M.; Verhoeff, N.P.L.G.; Kerwin, R.W. Antipsychotic Medication, D2 Dopamine Receptor Blockade and Clinical Response: A 123I IBZM SPET (Single Photon Emission Tomography) Study. *Psychol. Med.* **1993**, *23*, 791–797. [[CrossRef](#)] [[PubMed](#)]

80. Stone, J.M.; Davis, J.M.; Leucht, S.; Pilowsky, L.S. Cortical Dopamine D2/D3 Receptors Are a Common Site of Action for Antipsychotic Drugs—An Original Patient Data Meta-Analysis of the SPECT and PET In Vivo Receptor Imaging Literature. *Schizophr Bull.* **2009**, *35*, 789–797. [[CrossRef](#)] [[PubMed](#)]
81. Shokrzadeh, M.; Mohammadpour, A.; Modanloo, M.; Hassani, M.; Barghi, N.G.; Niroomand, P. Cytotoxic effects of aripiprazole on mkn45 and nih3t3 cell lines and genotoxic effects on human peripheral blood lymphocytes. *Arq. Gastroenterol.* **2019**, *56*, 155–159. [[CrossRef](#)]
82. Lemes, L.F.N.; Ramos, G.D.A.; Oliveira, A.; da Silva, F.M.R.; Couto, G.D.C.; Boni, M.D.S.; Guimarães, M.J.R.; Souza, I.N.D.O.; Bartolini, M.; Andrisano, V.; et al. Cardanol-derived AChE inhibitors: Towards the development of dual binding derivatives for Alzheimer's disease. *Eur. J. Med. Chem.* **2016**, *108*, 687–700. [[CrossRef](#)] [[PubMed](#)]
83. Limapichat, W.; Yu, W.Y.; Branigan, E.; Lester, H.A.; Dougherty, D.A. Key Binding Interactions for Memantine in the NMDA Receptor. *ACS Chem. Neurosci.* **2012**, *4*, 255–260. [[CrossRef](#)] [[PubMed](#)]
84. Farlow, M.R.; Graham, S.M.; Alva, G. Memantine for the Treatment of Alzheimer's Disease. *Drug Saf.* **2008**, *31*, 577–585. [[CrossRef](#)] [[PubMed](#)]
85. Stahl, S.M. Dopamine System Stabilizers, Aripiprazole, and the Next Generation of Antipsychotics, Part 2: Illustrating Their Mechanism of Action. *J. Clin. Psychiatry* **2001**, *62*, 923–924. [[CrossRef](#)] [[PubMed](#)]